CHAPTER 3
Establishing the O^6methyldeoxyGuanosine immunohistochemical assay

3.1. <u>Aim</u>

The specific aim with regard to setting up this methodology was as follows;

1. To establish a functional, consistent and reproducible immunostaining assay and image analysis system that allows the detection and quantification of O^6medG in rat colonic epithelial cells.

3.2. <u>Experimental Rationale</u>

The ability to be able to detect O^6medG DNA adducts in rat colonic tissue is fundamental to this project. Up to 6 different methods can be used for the detection adducts. These methods of detection include the use of immunoassays, gas or liquid chromatography and mass spectrometry, gel electrophoresis, electrochemical detection or atomic absorption [44, 169, 170]. Some of these methods however, are limited only to certain types of adducts, while other limiting factors include the amount of starting material and expense.

Due to these factors, it was decided that an immunoassay would be developed to detect O^6medG in rat colonic tissue. When using a stable, good quality antibody specific to the O^6medG adduct, this method has high specificity and sensitivity and is best suited to our particular requirements. Furthermore, the advantage of using an immunohistochemical assay to detect O^6medG in the colon is that the histological arrangement is retained and the distribution of adduct formation can be visualised along the colonic crypt at any time point following AOM administration. This is especially valuable in an area such as the colon as each crypt is lined with epithelial cells at different stages of maturity which play an important role in the initiation of CRC [28].

Though using this particular assay allows us to see which cells are affected, immunohistochemistry does have a disadvantage in that the final result can be

considered as more of a qualitative observation rather than quantitative. This however, can be overcome by the development of an image analysis system which allows us to measure colour and transfer it into a form of quantifiable data.

3.3. O^6medG immunohistochemical protocol

Pieces of distal colonic tissue were immediately placed into 10% buffered formalin following resection. After 18h of fixation, tissue pieces were transferred into 70% ethanol and were then processed overnight in an ethanol gradient and xylene (see Appendix B for details). Processed tissue was then embedded in paraffin wax and 4μm sections were cut and placed on poly-lysine coated slides to prevent loss of tissue during staining.

Sections were placed in a 37°C oven for 30mins to ensure tissue adherence to the slides. Following the heating of sections, they were deparaffinised in histoclear for 20mins with agitation. Sections were then rehydrated in a graded ethanol series (100%, 95%, 70% and 50%) for 2mins each and rinsed in dH$_2$O.

To block endogenous peroxidases, sections were placed in 3% H$_2$O$_2$ in 50% ethanol for 15mins and then rinsed in PBS.

A heat induced antigen retrieval method was used to undo any crosslinks in tissue formed by the formalin fixation. Sections were immersed in a 0.01M citrate buffer solution (pH 6.5). Sections were brought to the boil in a Sharp carousel microwave at full power for 1min and then left on low for a further 10mins. Sections were then left to cool in the citrate solution at room temperature for 30mins.

Tissue sections were rinsed with PBS and circled using a PAP pen. An RNase treatment comprised of RNase A (0.2mg/ml) and T (0.05U/ml) at was applied for 60mins at 37°C and then rinsed with PBS. This treatment degraded any RNA and ensured that only the methyl guanosine adduct on DNA was detected. A 140mM solution of NaCl was then added to the sections for 15mins at 4°C

followed by a PBS rinse. An alkali treatment of 60% 70mM NaOH/ 140mM NaCl and 40% methanol was then added to the sections for 5min at 4°C and immediately rinsed with PBS. This aided in denaturing the DNA and making it more susceptible to the antibody treatment [171].

A pre-block solution provided in the Acuity M.o.M. detection kit (Signet laboratories, 2706) was then used to cover the sections for 30mins at room temperature. Any excess solution was blotted off and a monoclonal primary antibody directed against O^6methyl-2-deoxyguanosine (Squarix biotechnology, clone EM 2-3, SQM003.1) was applied at a concentration of 0.1μg/ml. This solution was left on the sections over night at room temperature in a humidified chamber to prevent drying out.

The following morning sections were thoroughly rinsed (x3) with PBS. A post-block solution included in the Acuity M.o.M. kit was then applied to sections and left to incubate for 30mins. After rinsing with PBS (x3) the Poly-HRP anti mouse IgG solution was added for a further 30mins. This secondary linking 'biotin free' polymer gave greater sensitivity to the assay as well as ensuring that the problem of non-specific staining due to endogenous biotin was avoided. Following another serial rinse with PBS, the chromogen DAB was applied to tissues for 2mins and then rinsed in dH$_2$O thoroughly.

Sections were counterstained in haematoxylin for 1 min and rinsed well with dH$_2$O. Slides were then dunked briefly in 1% acid ethanol, rinsed thoroughly, dunked in 1% ammonia water and rinsed again in dH$_2$O. Slides were bought back through the ethanol gradient series (50%, 70%, 95% and 100%) for 2 mins each and were then placed in histoclear (x2) for 15mins and cover slipped.

Negative controls were including with every staining run. These included distal colonic tissue from a saline treated rat and colonic tissue from a rat killed 6h post AOM insult that was treated with PBS instead of the O^6medG primary antibody. An internal positive controlled was relied on for the tissues assayed. Positive staining appeared brown in colour and was restricted to the nuclei of colonic epithelial cells.

3.4.   Quantification of O^6medG immunoassay results

3.4.1. Scoring by eye

Prior to designing an image analysis method of quantification an alternative method was trialled which involved scoring the level of staining by eye. This method involved assigning each cell along the crypt length a score from 0 to 4 according to the degree of positive staining within the nuclei. The score of 0 represented a total absence of positive staining as observed in the negative controls, while a score of 4 corresponded to the darkest and most intense level of positive staining observed.

This technique was tested on 30 distal colonic crypts of a rat that had been treated with AOM 6h prior to resection. These specific sections were chosen as they appeared to have the greatest level of O^6medG staining and also the highest number of nuclei stained and therefore would be the most difficult to interpret.

This method produced satisfactory results in terms of representing the observed pattern of staining (see figure 6), however, this form of quantification proved to be quite tedious and time consuming and the consistency of measurement was in doubt. Though a clear scale of 0=no positive staining, 1=light positive staining, 2=medium positive staining 3=dark positive staining, 4=very dark positive staining was followed, it was difficult to retain the consistency between crypts and between sections. Furthermore, this scoring system would be difficult to account for the variability between runs that is inherent when using immunoassaying methods. Additionally, the interpretations of these levels of staining were likely to differ between users creating further potential problems.

Figure 6: O^6medG staining intensity counted by eye of a rat 6h post AOM
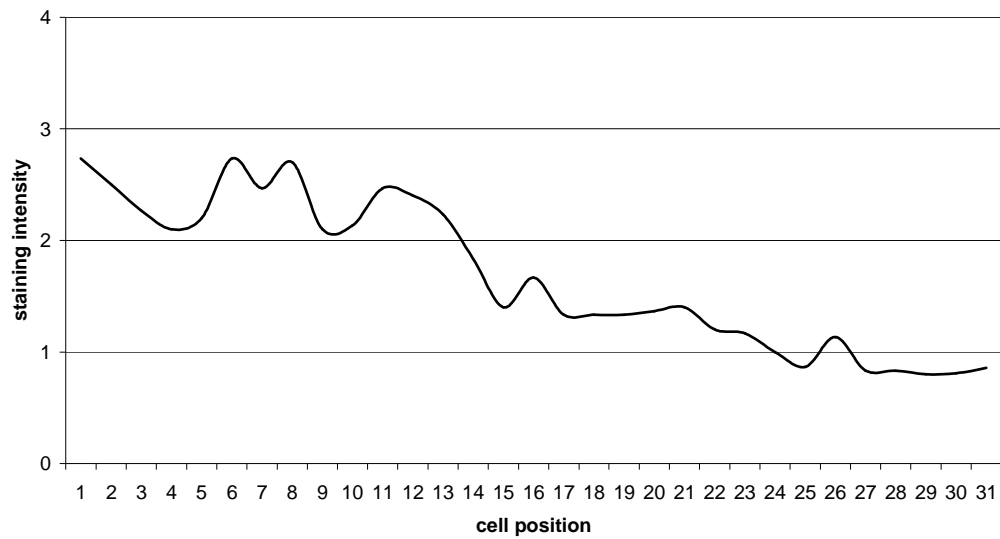
This graph displays the mean level of positive O^6medG staining in the distal colon of a rat 6h post AOM insult as counted by eye. The x-axis represents the intensity of the positive stain (0=no staining to 4=very dark staining); the y-axis represents the cell position in the crypt (1=base, 31=surface).

To confirm the concerns regarding the reproducibility of this method, the same method of O^6medG measurement was carried out in duplicate on a sample of distal colon from a second rat killed 6h post AOM. 30 crypts from were again randomly selected and the staining intensity for each cell was recorded.

The 2 sets of repeated counts were done in succession and the averages from both runs (A and B) are shown in figure 7. Though they display comparable patterns and have similar total O^6medG averages at 1.58 and 1.66 respectively, the slight inconsistencies between cell averages, particularly in the bottom proliferative zone of the crypt were enough to warrant investigations into establishing a more consistent and efficient quantification method using an image analysis system.

Figure 7: Comparing the mean O^6medG count done in duplicate along the colonic crypt of a rat 6h post AOM
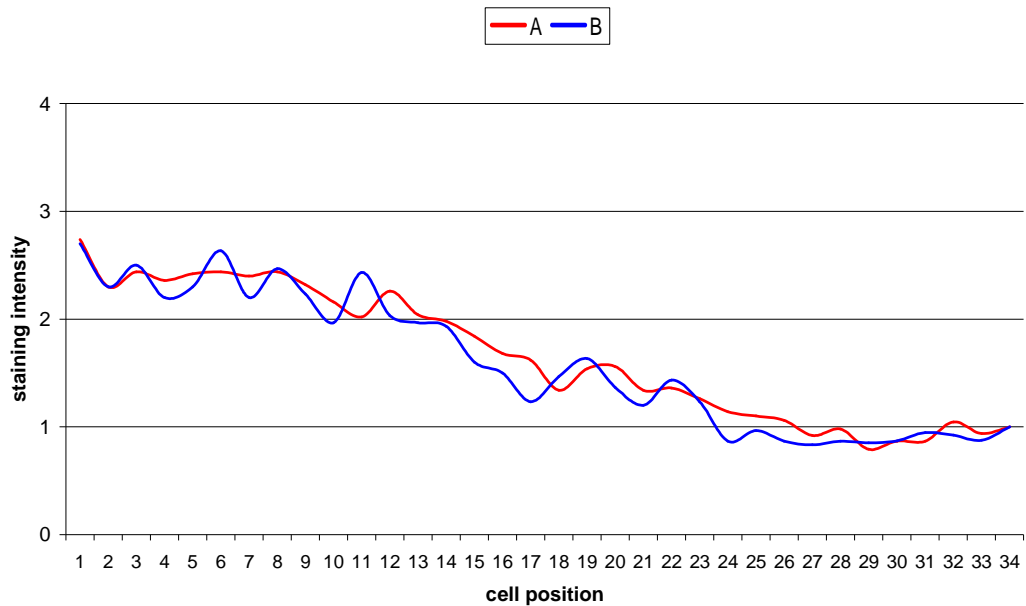
The graph displays the mean level of O^6medG positive staining in the same crypt. Counts were done by eye from a rat killed 6h post AOM insult. Counts were carried out in succession on the same 30 crypts. Staining intensity varied between counts for each nucleus and these inconsistencies warranted investigation into an alternative quantification method.

3.4.2. Image analysis system

The software used for the image analysis of the O^6medG staining was provided by Paul Jackway from the department of Mathematical and Information sciences, CSIRO. Using the program Olysia Bioreport Imaging System 5.0 for image capture and the programs 'R for windows', 2.1.0, and Q capture suite, 2.68.6.0, for image analysis a sound protocol was created which converted the level of positive staining for O^6medG seen visually into workable data points. The image analysis method was separated into 3 sections. These are detailed below.

3.4.2.1. Capturing the image

An Olympus BX-41 light microscope was used to locate the area of interest at 20x magnification. To ensure all microscope settings were consistent throughout the counting process a preset button was used each time which predetermined the intensity of the light source. Images of chosen crypts were photographed using an Olympus micropublisher 3.3 RTV camera and displayed using the Olysia

Bio-report software. Before these images were acquired the camera software was also calibrated to ensure consistency across all readings. The camera was white balanced before taking any images, exposure levels were set at a level of 3.381 and the RGB scale was set manually at 1.55(red), 1 (green) and 1.398 (blue) each time.

Once both the microscope and camera software were calibrated, duplicate images of 10 selected colonic crypts were captured and saved as Tiff files to ensure a high quality resolution. Colonic crypts were considered to be suitable for counting when the whole crypt was intact and had a distinct visible lumen with a row of single epithelial nuclei on either side from base to surface of the crypt as pictured in the figure 8.

Figure 8: An image of a colonic crypt deemed suitable for image analysis
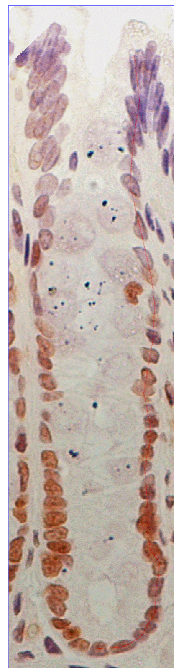
A suitable image taken of an entire and intact colonic crypt (from an animal killed 4h post AOM and stained for O^6medG) with no histological artefacts and a single row of epithelial cells either side of a distinct and open lumen.

3.4.2.2. Generating the data.

The captured images were opened using the 'R, 2.1.0' program in conjunction with the 'Q capture suite' program. This statistical software was developed by the 'R' foundation for statistical computing and essentially allowed the transformation of the colour and intensity of O^6medG staining into workable data points for each of the nuclei in the colonic crypts. It was decided that a variety of information about the colour and intensity of each stained section would be measured and recorded.

To begin with the area of interest within the crypt had to be identified. Beginning at the base of the crypt, this was done by clicking in the centre of each nucleus along the length of the crypt. At this time the numbers of cells comprising the crypt height were also counted and recorded. On the completion of identifying each nucleus, the program automatically drew a line through these points. Each pixel making up the length of the line represented one data point. Each data point had a series of information recorded which was automatically created in a CSV file as seen in figure 9 and described below.

Figure 9: CSV data file automatically created after identifying the line of interest in a crypt

An example of the CSV file containing data that are separated into columns and are relevant to each point along the drawn line in a single colonic crypt.

Each pixel which comprised the length of the line was assigned a number in column A and the three raw colours being red (Rd), green (Gd) and blue (Bd) were measured individually using the colour scale of 0-255. As these raw colours can be affected by light, such as the brightness of the microscope, luminescence (L) was also measured using the formula R + B + G. Normalised colour, represented by Rn, Gn or Bn, which accounts for the level of luminescence was also calculated and recorded using the formula Rn = Rd/L. As a blue colouration represented negative staining and brown represented positive, the two ratios accounting for red:blue and blue:green were also calculated and represented by RoB (Rn/Bn) and BoG (Bn/Gn).

Initially each piece of information was plotted to determine which best represented the staining pattern observed in the crypt. As shown below in figure 10, the 3 raw colours were similar in pattern, with only a slight separation of values occurring between the red and both the blue and green colours on areas of heavy positive staining. The luminescence line represented the amount of 'brightness' being measured. This level expectedly rose when measurements were taken towards the top of the crypt amongst the negative staining blue nuclei.

Figure 10: O^6medG image analysis red, green and blue raw data and luminescence counts
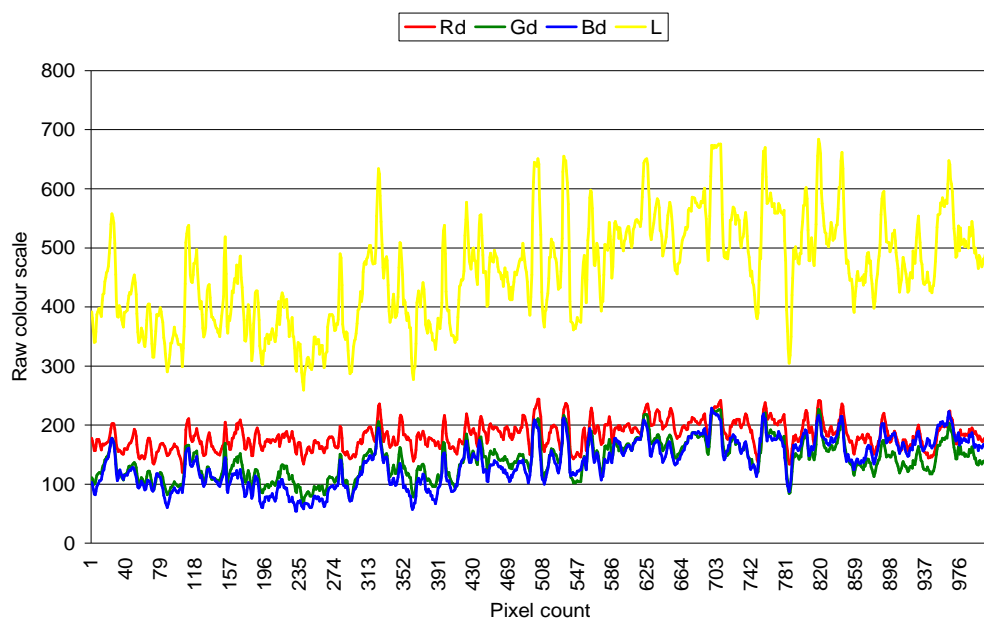
This graph displays the red, green, blue and luminescence values calculated from a crypt stained for O^6medG. Y-axis represents the colour scale; x-axis represents number of data points (or pixels) along the length of the drawn line.

Next, the raw values which had been adjusted for luminescence levels were plotted. While the pattern of green normalised values (see figure 11) does not differ that much from that shown in the raw data, both the blue and red normalised figures do take on a different pattern and hence, represent the positive staining observed in the crypt in a more accurate way with red values increasing at levels of intense positive staining while also being opposite to the blue levels measured.

Figure 11: O^6medG image analysis red, green and blue counts adjusted for luminescence
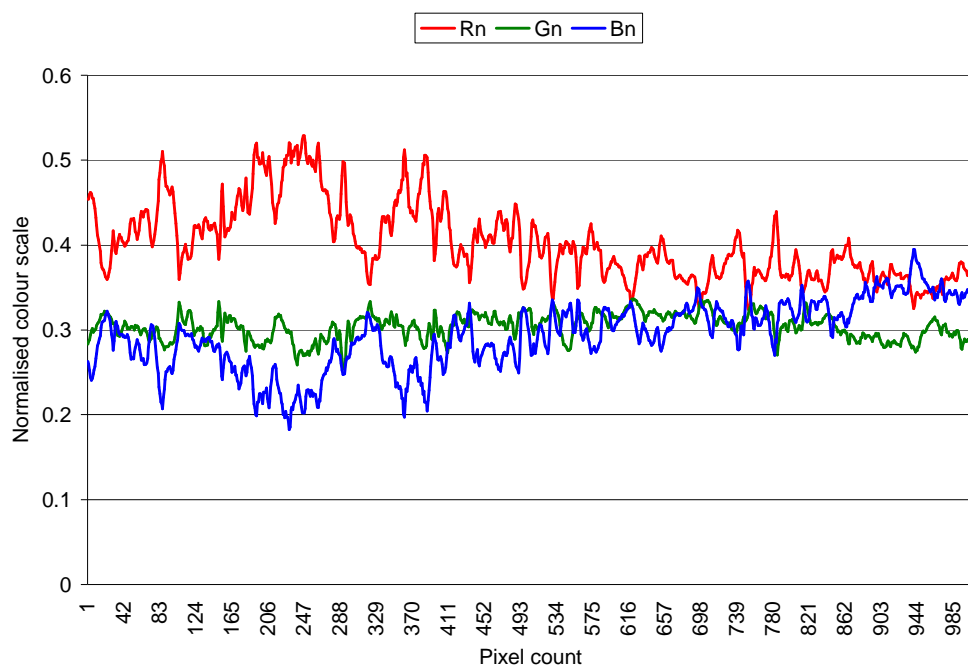
This graph shows the red, green, blue values normalised for luminescence. Y-axis represents the colour scale; x-axis represents number of data points along the length of the drawn line.

Lastly, the final pieces of ratio data were plotted (figure 12). This measure calculated the ratio from the normalised blue, green and red values to give the best representation possible. As shown in the graph below, the Blue: Green ratio measure did not display the appropriate pattern of staining, however, the Red: Blue ratio produce the best interpretation of the staining pattern as observed in the crypt. As a result it was decided that working with the RoB data would be the most appropriate as it most accurately characterized the staining pattern of crypts as observed by eye into representative data points.

Following this decision, this RoB data was used for an additional data set which was given the title 'fmeasure'. This function was added to give a smoothing effect to the plotted RoB data and this was done by calculating the average for every set of 51 measured data points along the length of the line using the 'measure' data in column K, which was simply a repeat of the RoB data. The additional 'fmeasure' average function also represented the staining pattern and intensity suitably.

Figure 12: O^6medG image analysis RoB and BoR ratio data and the measured RoB average
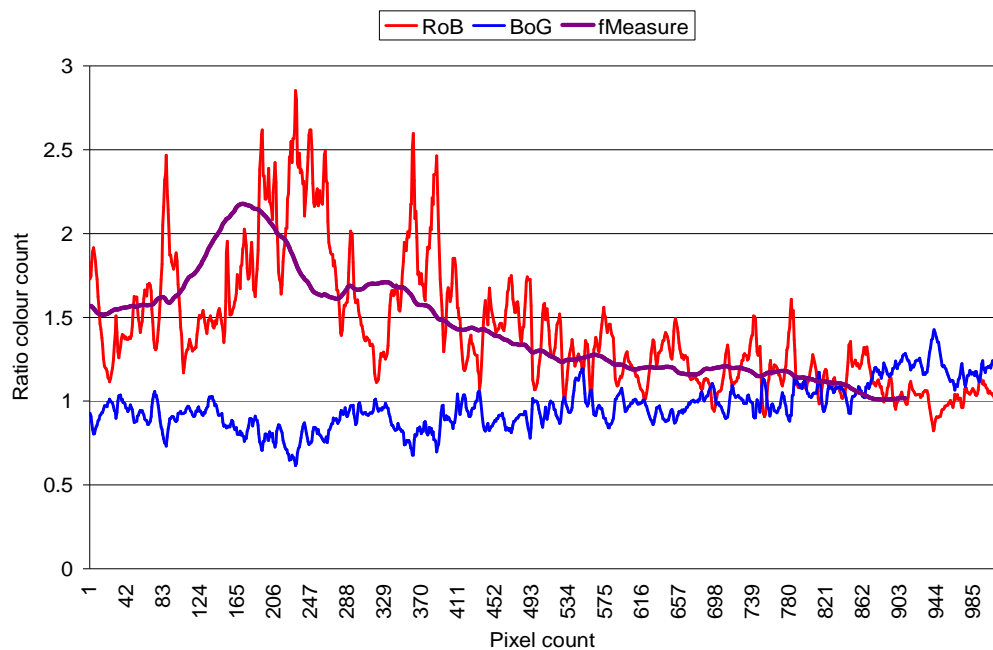
This graph shows the calculated colour ratios including the red: blue and blue: green values, an averaging function labelled as 'fmeasure' is also shown using the RoB data. Y-axis represents the colour scale; x-axis represents number of data points along the length of the drawn line.

This 'fmeasure' function was then trialled using a number of different set data points to determine if this averaging measure would be best suited to represent the staining patterns rather than using the raw RoB ratio data. 5 trials were done which averaged every set of 51, 150, 250, 350 and 450 RoB data points along the length of the line. The following graph (figure 13) shows the raw RoB data gained from each of the 5 trials using the same crypt. This not only demonstrates that the same values were used for this practice but also that when selecting the pathway through the nuclei, a consistent and uniform line can be repeatedly drawn. The second graph (figure 14) displays each of the 5 averaged counts. As

expected it is shown that as the data set used for averaging increases, both the length of the line shortens while the variation flattens out.

Figure 13: Repeated counts from a line drawn through the centre of nuclei from a crypt stained for O^6medG
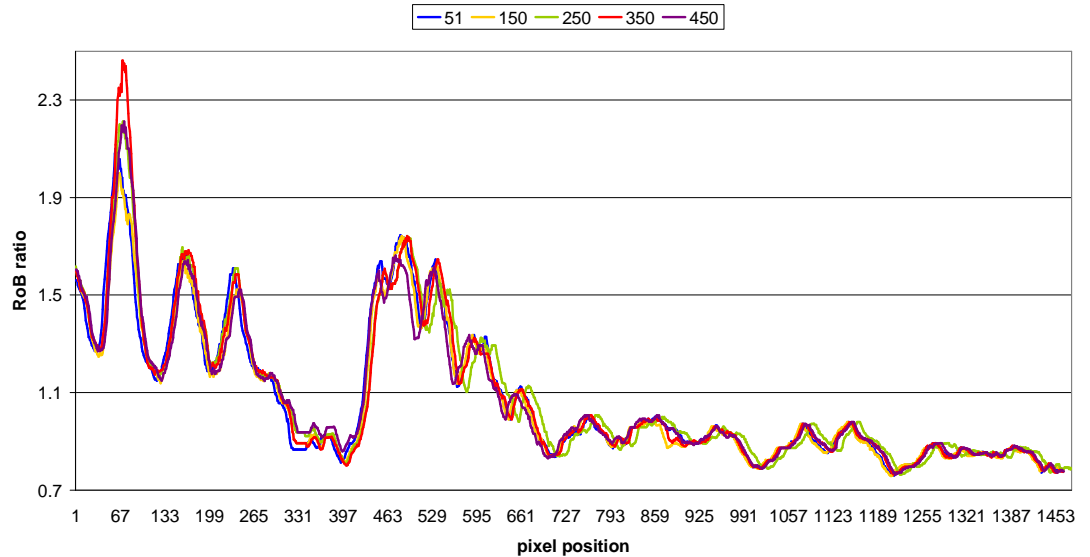
Repeated RoB ratio data calculated from 5 separately drawn lines through the middle of the nuclei from one stained crypt of interest. Each data set was used to test the validity of the 'fmeasure' function as shown in figure 14.

Figure 14: Adjusted RoB counts using the 'fmeasure' function with 5 different average boundaries
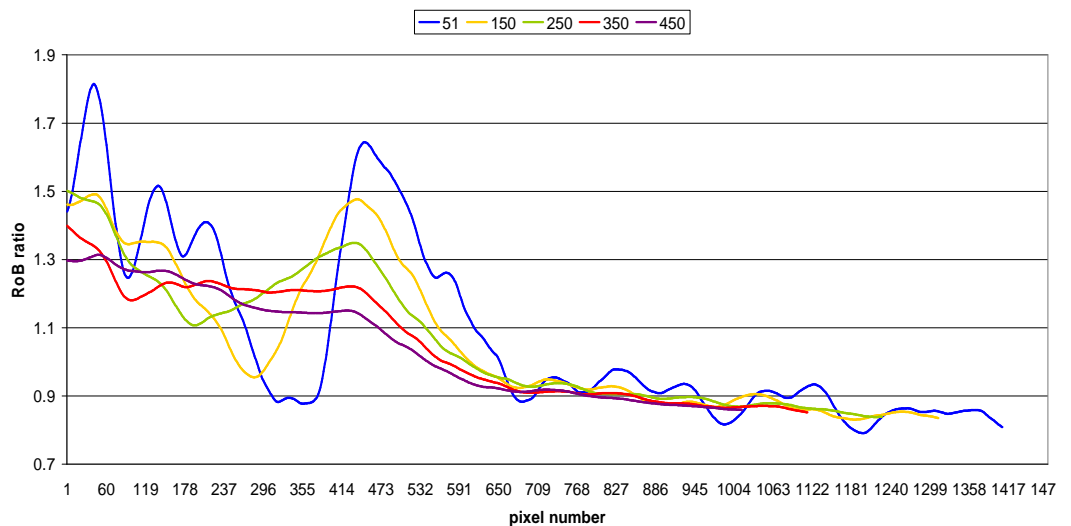
The 5 separate trials testing the validity of the 'fmeasure' function in best representing the Repeated RoB ratio data calculated from 5 individually drawn lines through the middle of the nuclei from one stained crypt of interest.

As a result of this smoothing effect and the loss of information within the crypt, it was decided that working with the raw RoB data and not an average measure of the RoB data would ensure that each staining pattern would be best represented with no data being lost or overlooked.

3.4.2.3. Organising the data.

Once these CSV files were created, the data from each file was simply copied and pasted into a prepared XLS template containing a number of prewritten functions. An example of the XLS template can be seen in figure 15 and the functions used in the template and their purposes are detailed below.

Figure 15: XLS template
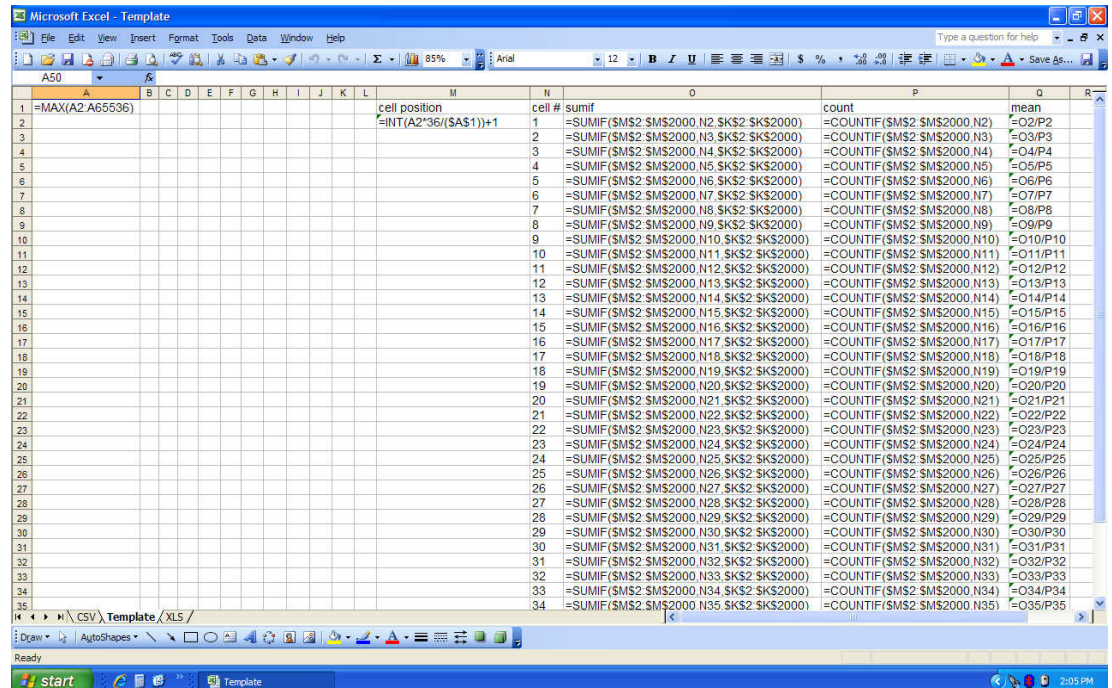
An example of the XLS template used to generate the final data needed from the initial CSV file. Data generated in each CSV spread sheet for every crypt was copied into this template and saved.

In A1 cell position the formula =MAX(A2:A65536) was used to calculate the number of data points in column A that were created or alternatively the length in pixels of the drawn line. The M2 cell contained the function =INT(A2*##/($A$1))+1. The ## figures were replaced with the cell height values for each crypt (for example, 36) and allowed the number of data points to

be grouped according to the number of cells present in the crypt, while Column N simply outlined the number of cells that made up the crypt length. The following formula =SUMIF($M$2:$M$2000,N2,$K$2:$K$2000) in column O calculated the sum of the RoB ratio data for all points in each cell position. The function =COUNTIF($M$2:$M$2000,N2) entered into column P simply calculated the number of data points that were assigned to each cell position.

This information was utilised in the final column which took the total sum of the RoB ratio for each cell position and divided it by the total number of data points assigned to that cell position (=O2/P2). This column then produced the final workable data set which best represented the mean colour RoB ratio for each nuclei along the length of a measured crypt. This final XLS sheet combining the raw CSV values and the specific formulas within the template is displayed in figure 16.

Figure 16: A CSV file pasted into the XLS template

An example of the final spreadsheet showing the generated CSV data in the XLS template. This resulted in the generation of the final data set (column Q) that gave a mean RoB value for each nucleus in a crypt that was measured.

An example of the average RoB ratio from a 6h post AOM stained crypt is represented by the line graph (figure 17) with the respective number of points used to calculate the average of each particular nucleus also displayed.

Though the scatter of certain values were greater than others, this was considered to be unavoidable at times when using this method as though the nuclei of the crypt were similar in size and shape, they were not uniform and the distances between each nuclei also varied. Therefore, when dividing the line length by number of cells, the scatter around some averages would at times be greater than others. The overall scatter however, was deemed to be an acceptable spread and one that did represent the data appropriately.

Figure 17: Average RoB data for each nucleus along the crypt length combined with the scatter of individual RoB counts for each nuclei
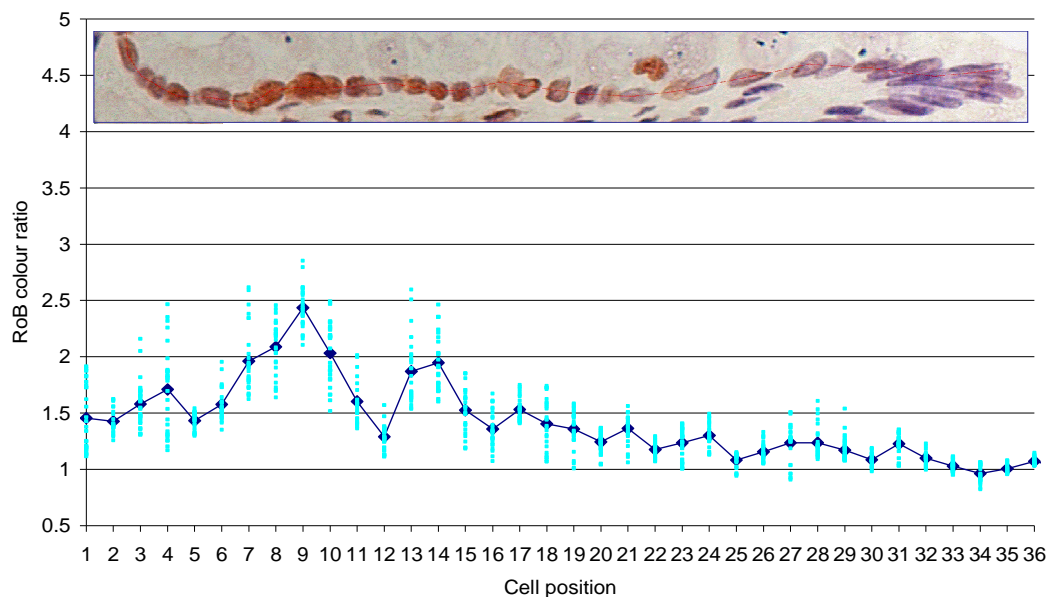
The dark blue line graph represents the mean of the staining ratio for each measured nucleus along the length of the pictured crypt. The light blue data points show the scatter of the data points used to generate the means for each nucleus.

When the average RoB ratio values for each nucleus in a crypt were added together, this equalled the total RoB ratio or in other words, the total level of positive staining (O^6medG) for each crypt. The mean RoB data can also be averaged by cell position across the 20 crypts measured for each rat. This then equates to an average level of O^6medG damage for each cell position along the length of a colonic crypt. Once these two forms of data were obtained from a

single rat it was then averaged with the RoB ratios measured in other rats in the same group to obtain a group average of O^6medG damage along the crypt and a total level of O^6medG.

Alternatively, the RoB ratio data for the nuclei of each individual crypt was also totalled to give a sum total of O^6medG damage. This value was then averaged for the 20 crypts in each rat and the 12 rats per group.

For all O^6medG data generated in this thesis, whether it is presented as an average value or a total level of damage, the background staining ratio established from the saline injected control groups was subtracted from the ratio data measured in all treatment groups. This ensured that all RoB staining ratios presented represented the actual level of O^6medG as accurately as possible.

3.5.   Camera comparison

The importance of retaining identical conditions for all image analysis measurements was reinforced from data gained using different cameras. Two different cameras of the same make and model (Olympus micropublisher 3.3 RTV) were used to measure the O^6medG level in both a saline treated control rat (figure 18) and a treated rat killed at 6h post AOM (figure 19). With each camera used the RGB scale, exposure and the white balance were set to ensure each trial was comparable. Image analysis of each sample was then carried out according to the described protocol.

As displayed in figure 18 and 19, though a similar pattern of staining was measured throughout the crypt with the 2 separate cameras, a difference was observed in the staining level represented as the RoB ratio.

This difference, though not significant in either the saline or AOM treated rat demonstrates how the process of quantifying immunostaining can be inaccurate if strict guidelines and protocols are not followed. As a result of this data, only one camera and the appropriate corresponding hardware were used during the analysis of all samples measured for O^6medG in this thesis.

Figure 18: Comparison of RoB ratio from saline control colonic crypt for different camera settings
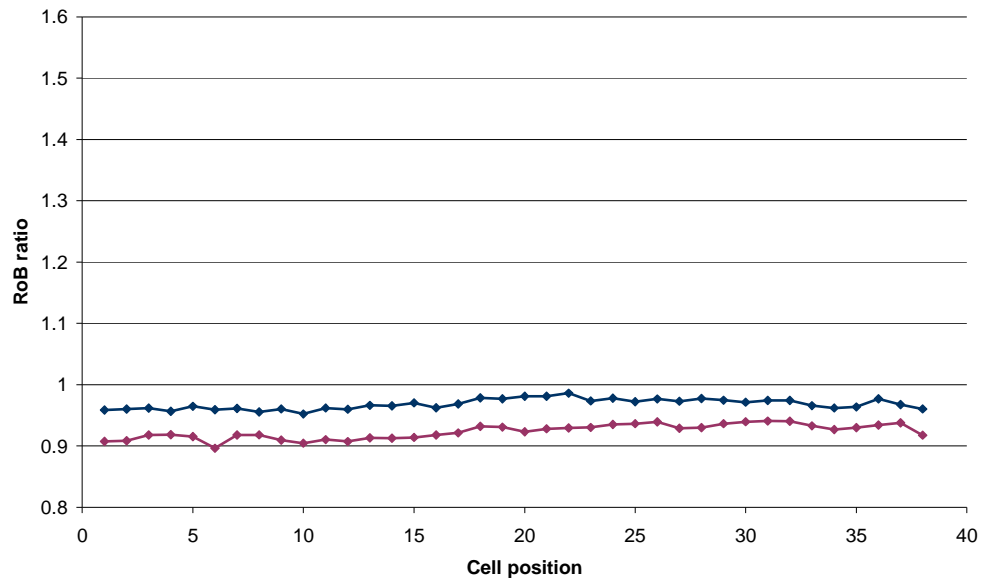
Level of RoB staining in the same sample from a saline control rat using two different cameras. All software settings and camera settings were identical for each image analysis trial (blue =camera A, Purple =camera B)

Figure 19: Comparison of RoB ratio from AOM treated colonic crypt for different camera settings
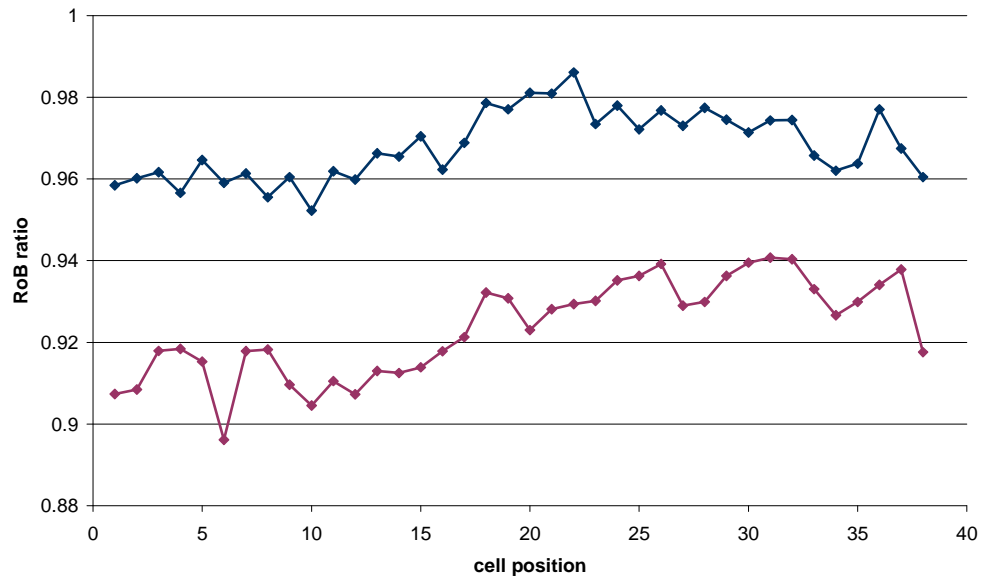
Level of RoB staining in the same sample from an AOM treated rat using two different cameras. All software settings and camera settings were identical for each image analysis trial (blue =camera A, Purple =camera B)

3.6.   <u>Summary</u>

The need to establish a functional and reproducible assay for the measurement of acute O^6medG DNA damage was essential for the completion of this thesis.   It was decided that an immunochemical assay would be established not only due to the high sensitivity and specificity that it could deliver but also as a result of being able to identify the actual distribution of these adducts in colonic crypts.

A protocol was designed, tested and refined in order to give clear and specific positive staining results while retaining a minimal level of interference from background staining. All steps included in the protocol were tested for the optimal time and temperature of incubation or the concentration of reagents used. The primary antibody in particular was set at a concentration of 0.1μg/ml as this gave optimal staining conditions. The protocol was trialled with individual blocking serums and secondary antibodies, however, the Signet Acuity M.o.M. kit containing the secondary polymer linking technology gave superior staining results and was therefore used in the protocol for the assaying of all samples in this body of work.

Once the O^6medG immunoassay was established and was producing consistent results, the method of quantifying this data was investigated. Scoring the level of staining in colonic nuclei was attempted by eye but was deemed too inconsistent and time consuming. Therefore, an image analysis system of quantification was developed.

The process of this controlled image analysis system involved capturing an image of a suitable colonic crypt stained for O^6medG under the microscope. After identifying an area of interest, the image analysis software then converted the colour of the specified area into a series of data points. The raw colours, the level of luminescence, the normalised colours and a series of colours ratios were provided for each data point. After analysing these data and comparing it to the staining pattern as observed by eye, it was established that the Red: Blue ratio would be used to best describe the distribution and intensity of nuclei positively stained for O^6medG.

Once this was established, the data was sorted using statistical means to best represent the level of O^6medG per epithelial cell in a crypt and when summed, a total level of O^6medG load per crypt.

Both the immunostaining assay and the image analysis method of quantification were thoroughly tested on a variety of samples. These results, supported by acceptable negative control samples, were deemed to be reproducible and reliable enough to carry on with the analysis of colonic tissue samples from both the time course and dietary intervention studies.